Supplementary Information

Fluoranthene based fluorescent chemosensors for detection of explosive nitroaromatics

N. Venkatramaiah, Shiv Kumar and Satish Patil*

Solid State and Structural Chemistry Unit, Indian Institute of Science,Bangalore-560012, India. Fax: +91-80-23601310; Tel: +91-80-22932651E-mail: satish@sscu.iisc.ernet.in

General procedure

All chemicals were purchased from Sigma Aldrich and used without further purification. ^{1}H NMR, ^{13}C NMR spectra were recorded on Bruker 400 MHz NMR spectrometer and calibrated using TMS as an internal reference. Chemical shifts are reported in parts per million (ppm).

1. Synthesis and characterization of S_1

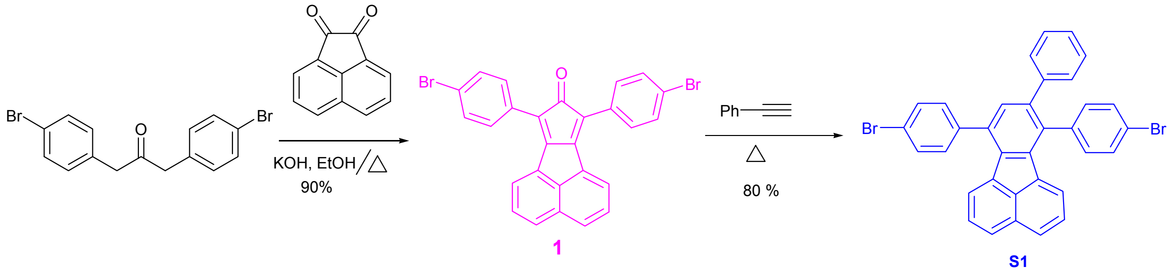

Synthesis of 7,10- bis(4-bromophenyl)-8H-cyclopenta[*a*]acenaphthylen-8-one (1)

The compound **1** was synthesized by Knoevenagel condensation between 1,3-bis(4-bromophenyl)propan-2-one (0.933 g, 3 mmol) and Acenapthenedione(0.546g, 3 mmol) in 5 mL of ethanol medium. KOH (0.095g) in 2mL ethanol was added drop wise and the mixture was refluxed for 15 min. under heating. The reaction mixture was cooled to 0 °C and the purple color solid was filtered. The obtained compound was insoluble in common solvents.

Synthesis of 7,10-bis(4-bromophenyl)-8-phenylfluoranthene (S_1)

A 15 mL pressure glass tube was charged with 7,10- bis(4-bromophenyl)-8H-cyclopenta[*a*]acenaphthylen-8-one (0.102 g, 0.2 mmol) and phenylacetylene (30µL, 0.28 mmol) to which a minimal amount (ca. 1.5 mL) of 1,2,4 trichlorobenzene was added. It was degassed by bubbling argon and sealed. The heterogeneous purple-black solution was heated to 220 °C with vigorous stirring until it became homogeneous and gives transparent greenish yellow colour. The reaction mixture was cooled in an ice bath and diluted with hexane to precipitate the crude product, which was collected by filtration and washed with copious amounts of ethanol. The resulting pale yellow solid was then purified by passing it through silica gel column in 4:1 hexane/ethylacetate mixture as eluent yielding pure $\mathbf{S_1}$ (92 mg, 80% yield). ^{1}H NMR (400 MHz, $CDCl_3$) δ 7.77 (t, J = 7.3 Hz, 2H), 7.69 (d, J = 7.9 Hz, 2H), 7.55 (dd, J = 17.4, 8.0 Hz, 4H), 7.42 (t, J = 7.6 Hz, 2H), 7.34 (dd, J = 16.4, 7.5 Hz, 2H), 7.26 – 7.16 (m, 9H), 6.77 (d, J = 7.1 Hz, 1H). ^{13}C NMR (400 MHz, $CDCl_3$) δ 140.87, 140.49, 139.53, 138.16, 136.81, 136.13, 135.70, 135.45, 135.06, 133.04, 132.06, 133.04, 132.06, 131.87, 131.73, 131.10, 130.95, 130.83, 130.30, 129.85, 127.98, 127.78, 127.73, 127.64, 127.01, 126.64, 123.37, 122.96, 122.07, 121.54. CHN analysis: Calculated: C, 69.41; H, 3.43; Br, 27.16, Found: C, 69.41; H, 3.98; Br, 26.51.

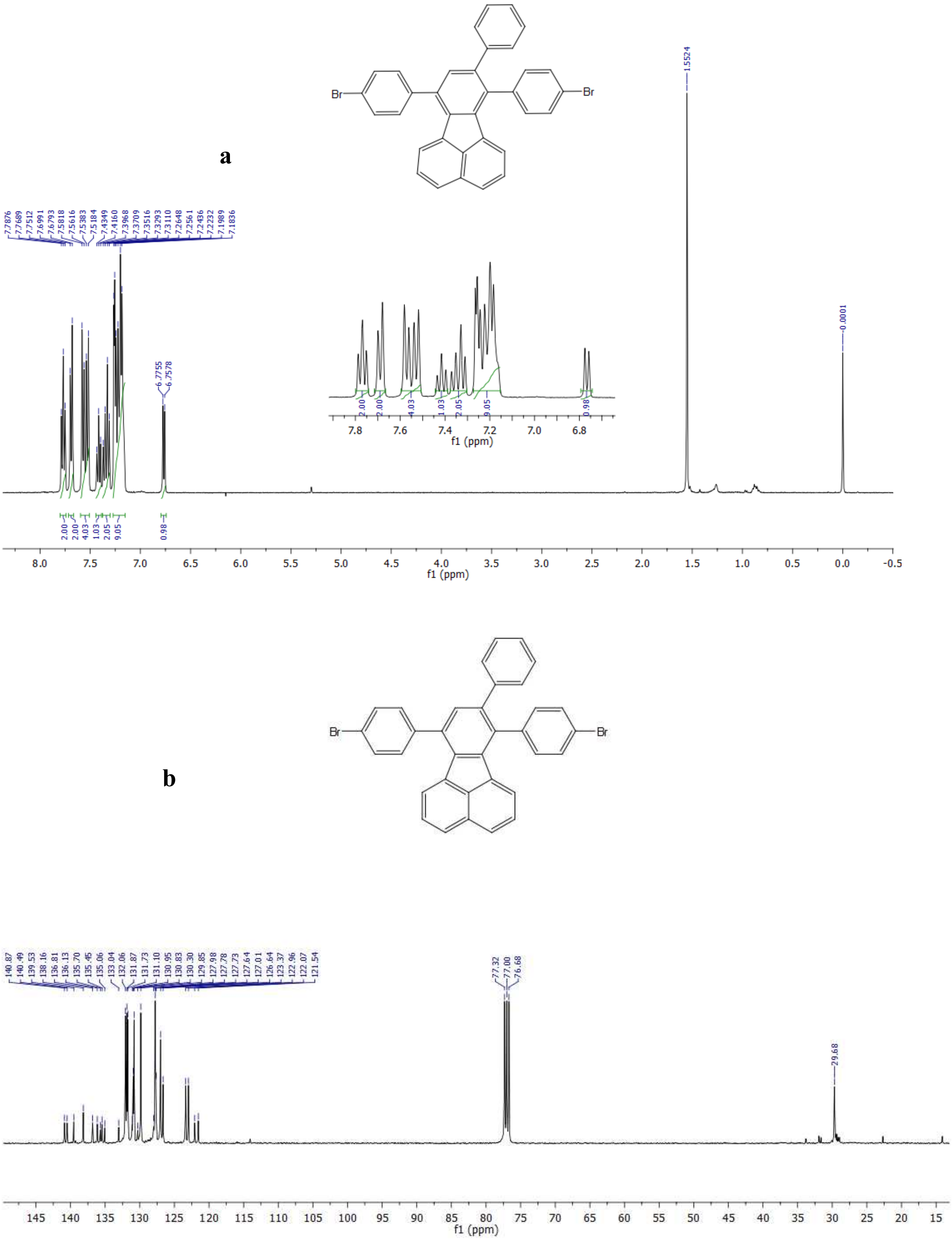

Fig.A1 The ^{1}H NMR (a) and ^{13}C NMR spectra of $\mathbf{S_1}$ in $CDCl_3$.

2. Single crystal X-ray analysis

Single crystal X-ray diffraction data was collected at 120 K on an Oxford Xcalibur (Mova) diffractometer equipped with a EOS CCD detector using *MoKα* radiation (λ= 0.71073Å).[1] The crystal was maintained at the desired temperature during data collection using the Oxford instruments Cryojet-HT controller. The structure was solved by direct methods using SHELXS-97 and refined against F2 using SHELXL-97.[2] H-atoms were fixed geometrically and refined isotropically. The WinGX package was used for refinement and production of data tables, and ORTEP-3 for structure visualization and making molecular representations showing the ellipsoids at 50% probability level.[3]

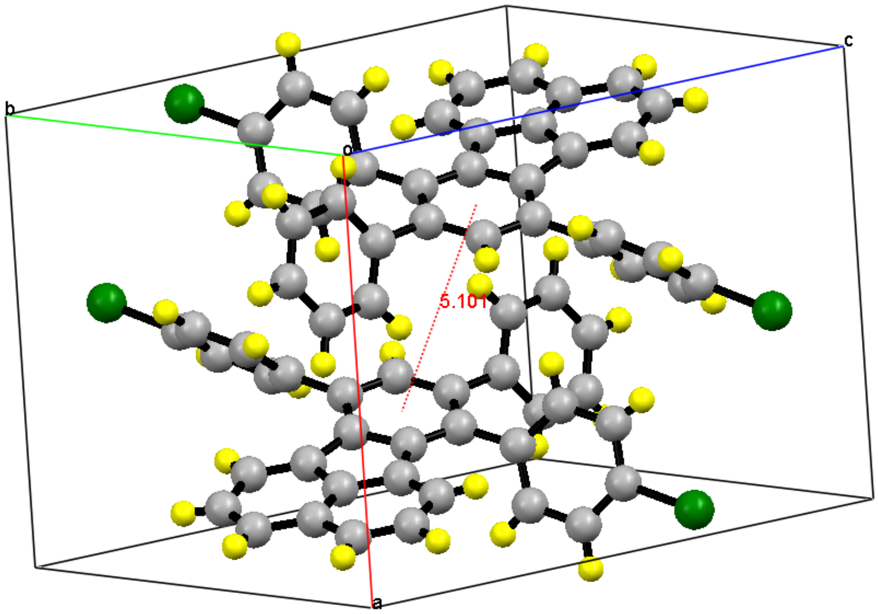

Fig.A2 Unit cell packing diagram of $\mathbf{S_1}$ viewed along the *b*-axis.

Table 1. Crystal data and structure refinement parameters for **S_1**.

Compound	**S_1**
Formula	$C_{34}H_{20}Br_2$
Formula weight	588.3
Crystal system	Triclinic
Space group	*P*-1
a (Å)	10.3812(7)
b (Å)	10.9799(8)
c (Å)	12.2684(9)
Volume (Å^3)	1236.68(53)
Z	2
Density (gcm^{-3})	1.58
μ (mm^{-1})	3.300
F (000)	587.9
$h_{min, max}$	-13,13
$k_{min, max}$	-14,14
$l_{min, max}$	-15,15
No. of measured reflections	21125
No. of unique reflections	5370
No. of reflections used	3828
$R_{\_all}$, $R_{\_obs}$	0.089, 0.057
wR_{2_all}, wR_{2_obs}	0.163, 0.147
$\Delta\rho_{min,max}$ (e Å^{-3})	0.163, 0.147
GOOF	1.010

3. Fluorescence quenching with different nitroaromatics in ethanol solution

Steady-state fluorescence emission studies were carried out with Spex FluoroLog-3 spectrofluorometer (Jobin-Yvon Inc.).

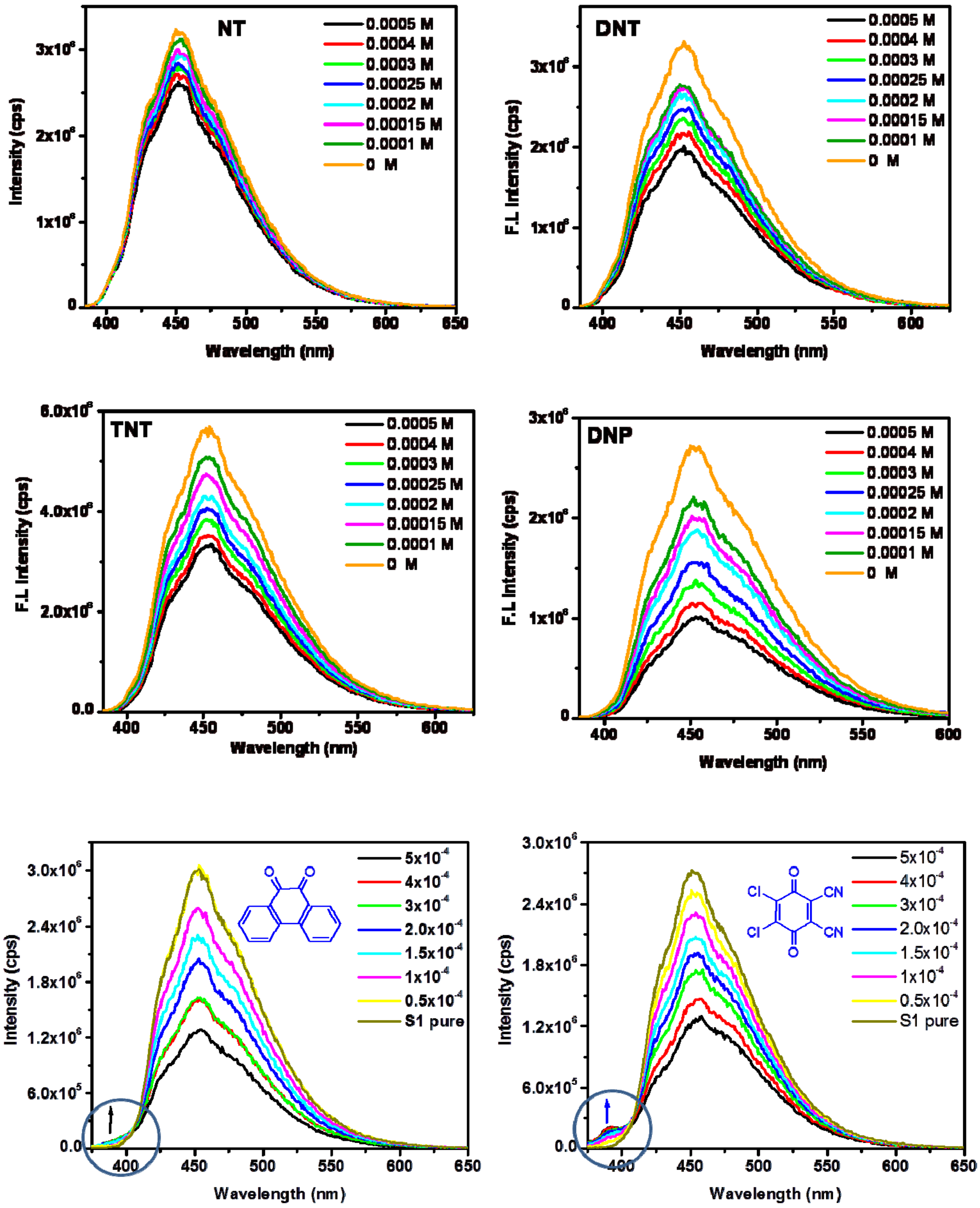

Fig. A3 The spectrofluorometric addition of different concentrations of various nitroaromatics to **S₁** (1x10^{-6}, M) in ethanol at 25˚C. The circles indicate the formation of new emission peak upon addition of PAQ and DDQ to **S₁**. NT: 4-nitro toluene, DNT: 2,4 dinitrotoluene, TNT:2,4,6 trinitrotoluene,DNP: 2,4 dinitrophenol

4. Stern-Volmer plots

The quenching behavior was studied by Stern-Volmer equation Io/I=1+K_{sv}[Q], where I_o, I are the fluorescence intensity before and after addition of the quencher, K_{sv} is the Stern-Volmer quenching rate constant and [Q] is the concentration of the quencher. Linear SV response was observed for common analytes indicating static quenching behaviour. However, the highly electron deficient compounds like DDQ, PAQ chloronil and ANQ shows non-linear behaviour at high concentration suggesting that the fluorescence quenching of $\mathbf{S_1}$ follows both static as well as dynamic quenching pathways through the ground state complex formation.

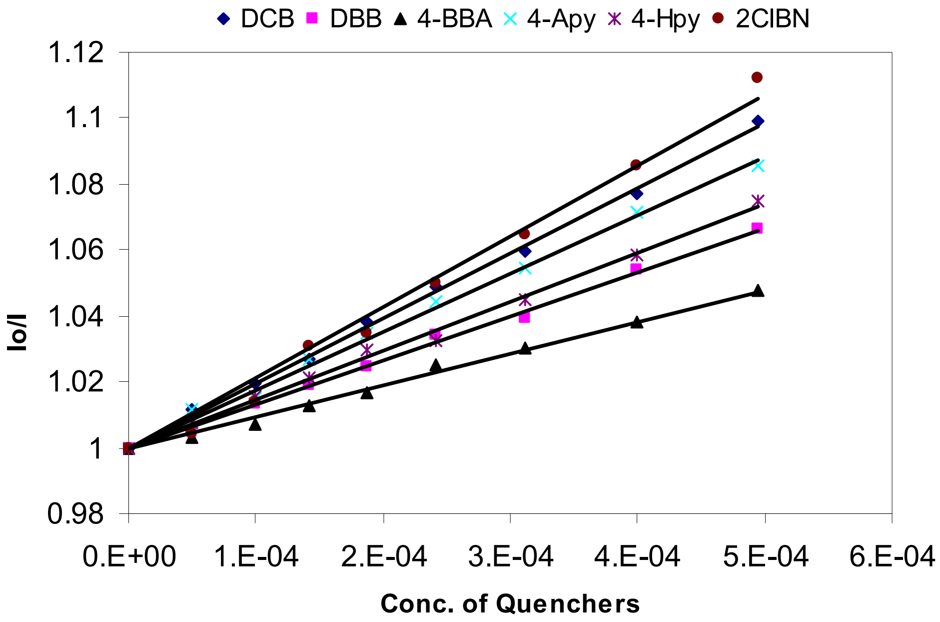

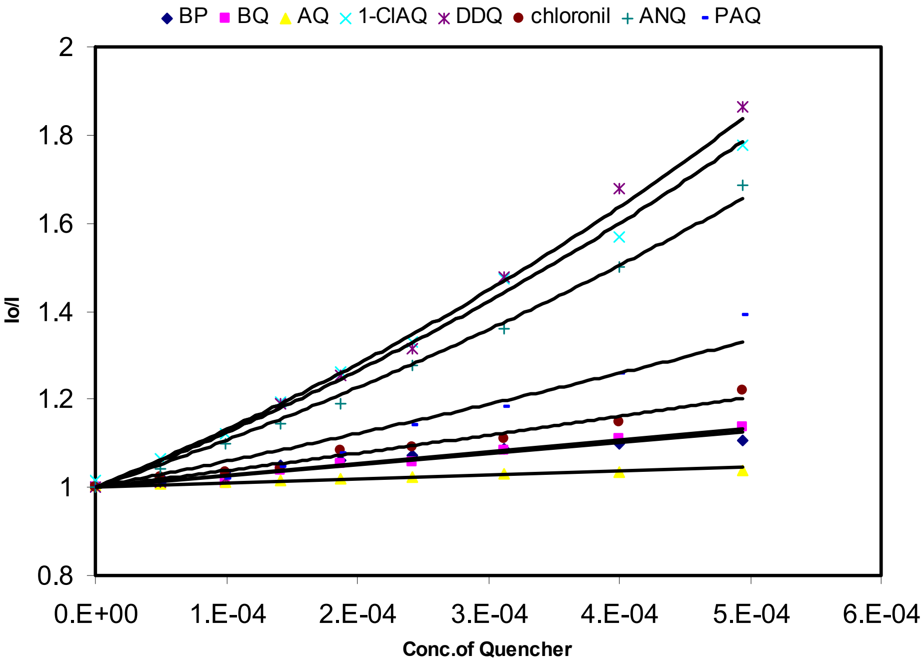

Fig. A4 The Stern-Volmer plots for different concentrations of various analytes. The curves for DDQ, ANQ, Chloronil and 1-ClAQ shows presence of both static and dyanmica quenching when treated with $\mathbf{S_1}$.

5. Time resolved fluorescence

Time resolved fluorescence measurements were carried out with time-correlated single-photon counting (TCSPC) using nanosecond LED (459 nm, FWHM≤1.3 ns) with repetition rate of 1 MHz to excite the samples. The photons collected at the detector are correlated by time-to-amplitude converter (TAC) to the excitation pulse. Signals were collected using an IBH data station Hub photon counting module and data analysis was performed using the commercially available DAS6 software (HORIBA JobinYvon IBH).

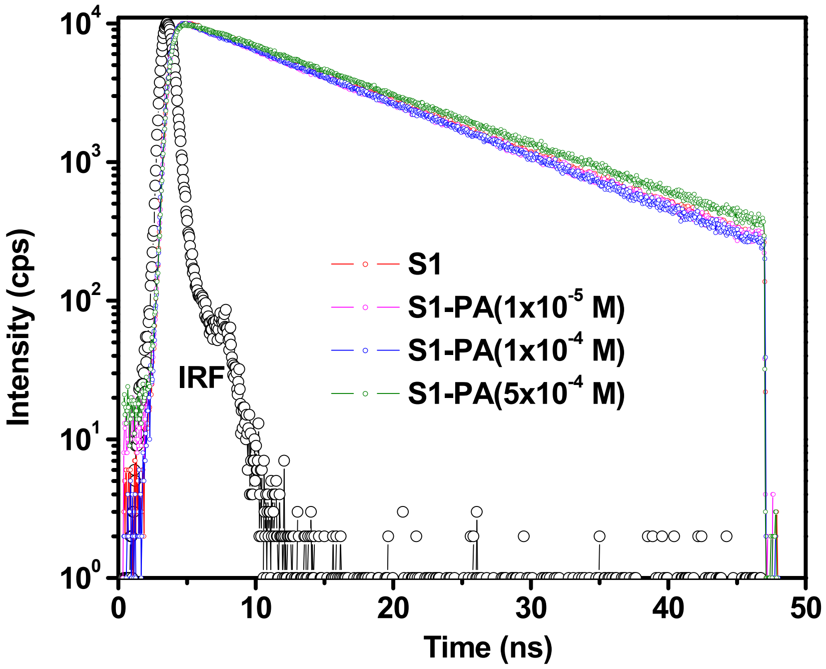

Fig.A5 Time resolved fluorescence emission spectra of **S_1** for different concentrations of PA

6. Optical absorption

The UV–Vis spectra were recorded on Perkin-Elmer (Lambda 35) UV–Vis Spectrometer. All the spectra in solution were recorded in $CHCl_3$ and the spectra in the solid state were recorded using 1mg of S1 in 0.2 mL $CHCl_3$ solution spin coated on quartz plates.

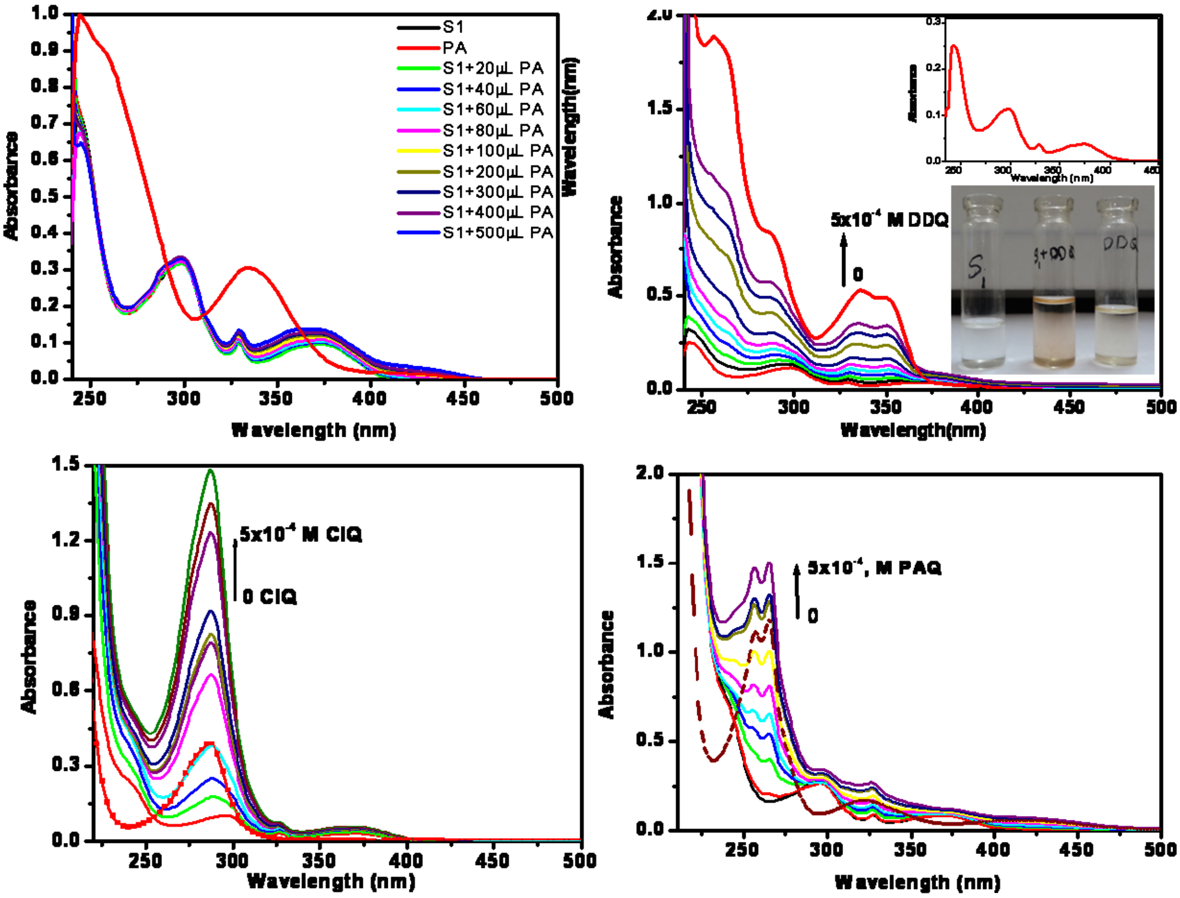

Fig. A6 Optical absorption spectra of $\mathbf{S_1}$ ($5x10^{-5}$ M) upon addition of different concentration of PA (0.1mM) in ethanol solution

7. Selectivity

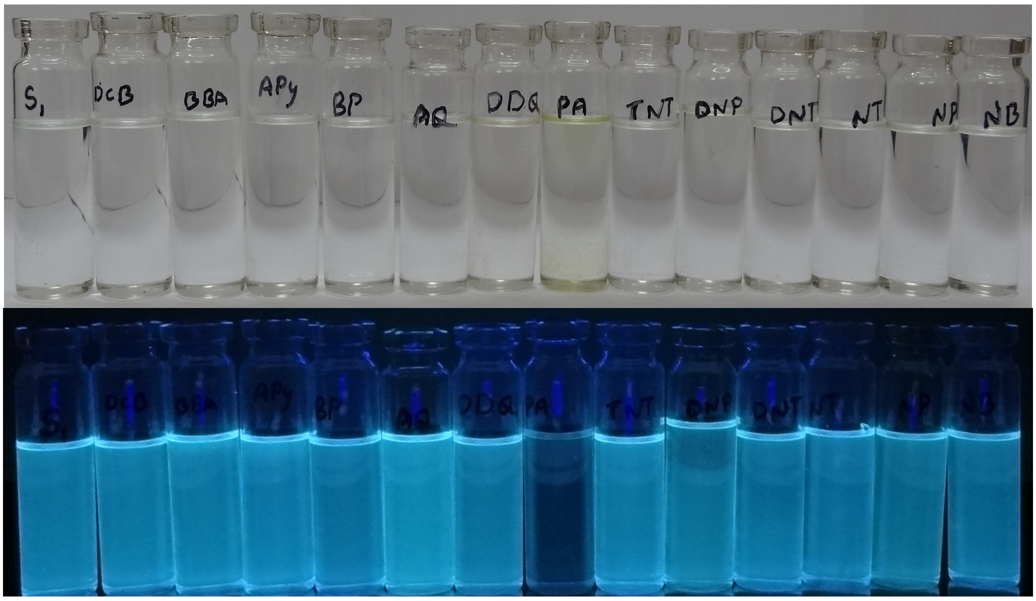

Fig.A7 The change in the fluorescent intensity of **S_1** upon addition of 10 μL of various analytes before and after exposure to the UV light at 365 nm. DCB (1,4-dichloro benzene), BBA(4-bromo benzoic acid), APy (4-amino Pyridine), HPy(4-hydroxy Pyridine), BP(benzophenone), AQ(anthraquinone), DDQ (2,3 dichloro 5,6-dicyano 1,4-benzoquinone), PA(picric acid),TNT(2,4,6-trinitrotoulene), DNP(2,4,6-trinitro phenol), DNT (2,4,-dinitrotoulene), NT (4-nitro toluene), NP(4-nitro phenol) and NB (nitro benzene).

8. Solid state fluorescence quenching with saturated vapors different nitroaromatics

Saturated vapors of different nitroaromatics were generated by keeping the compounds in a sealed tube for three days to ensure that the equilibrated vapor pressure is reached. The solid state fluorescence quenching study was carried out by keeping the quartz plate in sealed tubes for specific time. The fluorescence spectra of the exposed films were recorded immediately after taking out from the sealed tube without any delay.

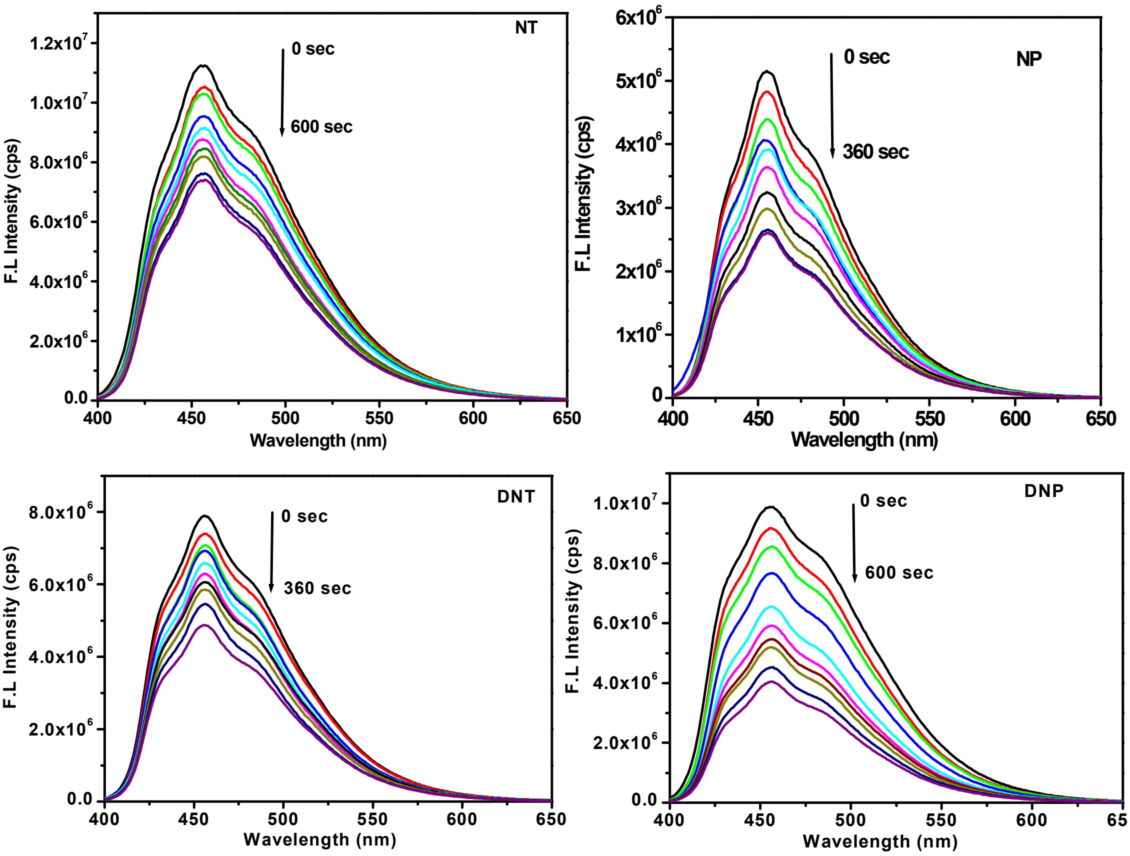

Fig. A8 The time dependent emission spectra of **S$_1$** thin film upon exposure to saturated vapors of various nitroaromatics at 60 sec interval of time.

9. Solid state quenching efficiency towards the saturated vapors of nitroaromatics

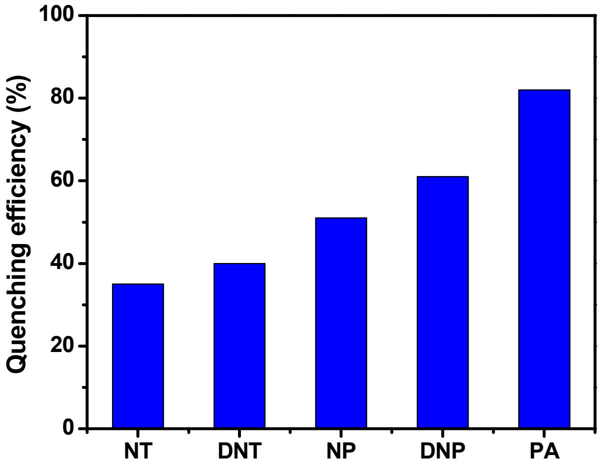

Fig.A9 Fluorescence quenching efficiency of **S_1** thin film to the saturated vapors of various nitroaromatics for 120 sec of exposure time.

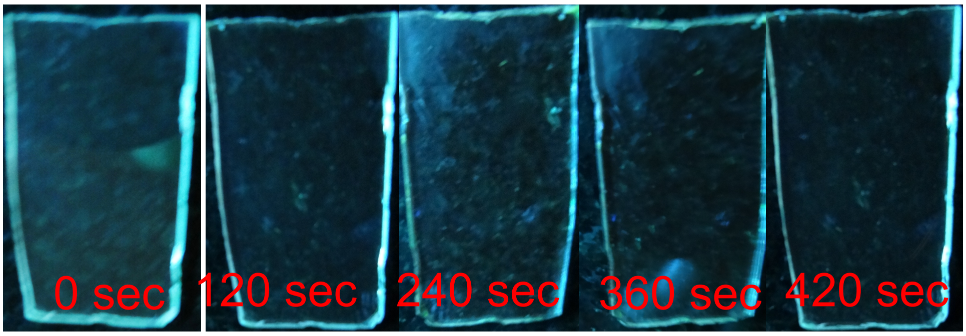

Fig.A10 A representative fluorescence quenching of **S_1** thin film to the saturated vapors of Picric acid for every 120 sec of exposure time.

9. Computational study

The molecular structure of **S_1** was optimized in Gaussian 03 with 6-31g* as basis set.[4] Electron density distribution of highest occupied molecular orbital (HOMO) and lowest unoccupied molecular orbital (LUMO) are generated from the optimized structure. The energy level diagram was generated from the HOMO and LUMO of S_1 with redox potentials of different NACs.

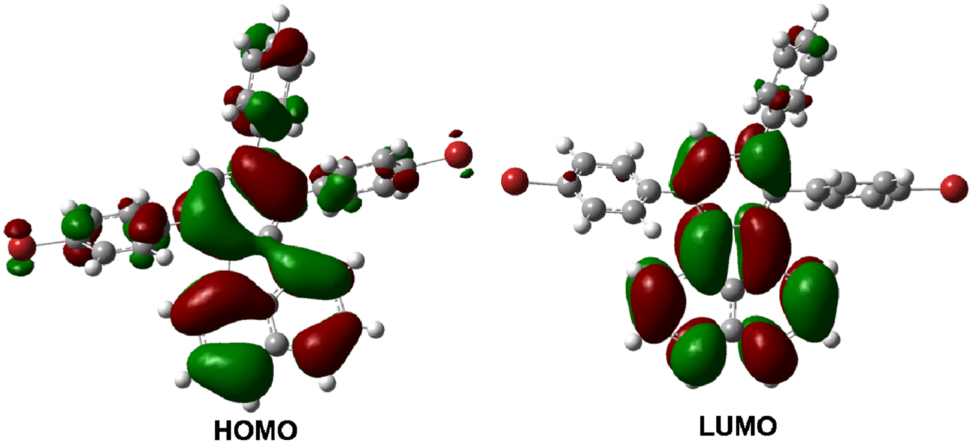

Fig.A11 The electron density profiles of **S₁**

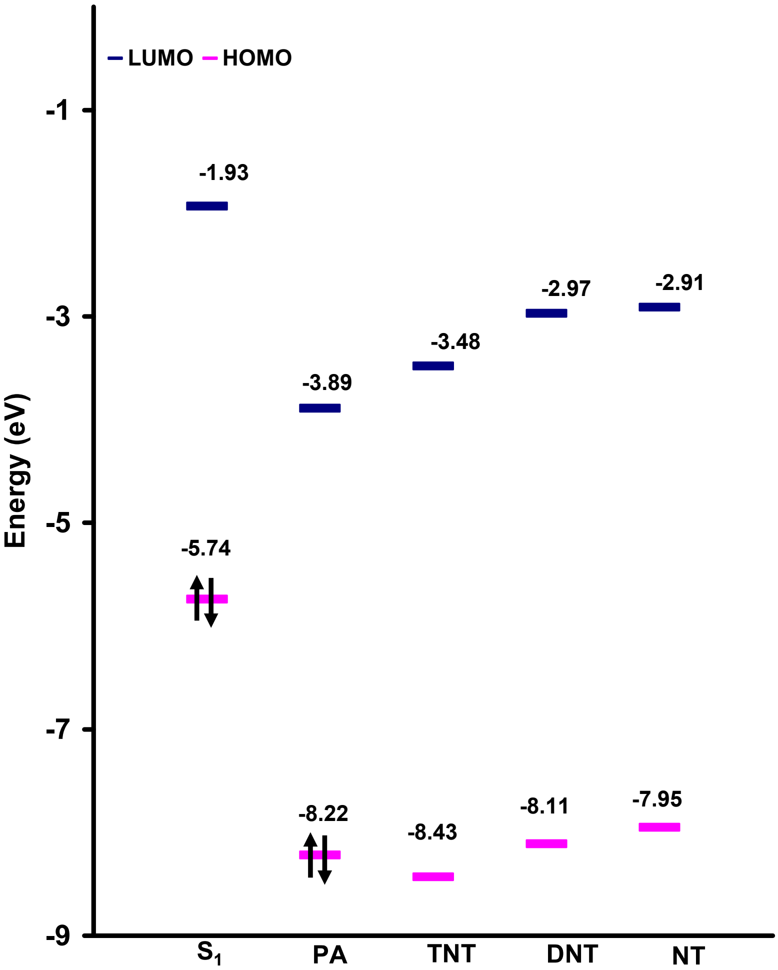

Fig.A12 The energy level diagram of **S₁** with other nitroaromatics.

References:

1. Oxford Diffraction (2009). *CrysAlis CCD and CrysAlisPro RED*, Version 1.171.33.34d. Oxford Diffraction Ltd., Abingdon, Oxfordshire, England.
2. G. Sheldrick, *Acta Crystallogr., Sect. A: Found. Crystallogr.*, 2008, **64**, 112–122.
3. L. Farrugia, *J. Appl. Crystallogr.*, 1999, **32**, 837–838.
4. M. J. T. Frisch, G. W. Trucks, H. B. Schlegel, G. E. Scuseria, M. A. Robb, J. R. Cheeseman, J. A. Montgomery, Jr., T. Vreven, K. N. Kudin, J. C. Burant, J. M. Millam, S. S. Iyengar, J. Tomasi, V. Barone, B. Mennucci, M. Cossi, G. Scalmani, N. Rega, G. A. Petersson, H. Nakatsuji, M. Hada, M. Ehara, K. Toyota, R. Fukuda, J. Hasegawa, M. Ishida, T. Nakajima, Y. Honda, O. Kitao, H. Nakai, M. Klene, X. Li, J. E. Knox, H. P. Hratchian, J. B. Cross, V. Bakken, C. Adamo, J. Jaramillo, R. Gomperts, R. E. Stratmann, O. Yazyev, A. J. Austin, R. Cammi, C. Pomelli, J. W. Ochterski, P. Y. Ayala, K. Morokuma, G. A. Voth, P. Salvador, J. J. Dannenberg, V. G. Zakrzewski, S. Dapprich, A. D. Daniels, M. C. Strain, O. Farkas, D. K. Malick, A. D. Rabuck, K. Raghavachari, J. B. Foresman, J. V. Ortiz, Q. Cui, A. G. Baboul, S. Clifford, J. Cioslowski, B. B. Stefanov, G. Liu, A. Liashenko, P. Piskorz, I. Komaromi, R. L. Martin, D. J. Fox, T. Keith, M. A. Al-Laham, C. Y. Peng, A. Nanayakkara, M. Challacombe, P. M. W. Gill, B. Johnson, W. Chen, M. W. Wong, C. Gonzalez and J. A. Pople, *Gaussian 03, revision C.02*, Gaussian Inc., Wallingford, CT, 2004.